Rate Maximization for Downlink Pinching-Antenna Systems

Yanqing Xu, *Member, IEEE,* Zhiguo Ding, *Fellow, IEEE,* and George K. Karagiannidis, *Fellow, IEEE*

***Abstract*—In this letter, we consider a new type of flexible-antenna system, termed *pinching-antenna*, where multiple low-cost pinching antennas, realized by activating small dielectric particles on a dielectric waveguide, are jointly used to serve a single-antenna user. Our goal is to maximize the downlink transmission rate by optimizing the locations of the pinch antennas. However, these locations affect both the path losses and the phase shifts of the user's effective channel gain, making the problem challenging to solve. To address this challenge and solve the problem in a low complexity manner, a relaxed optimization problem is developed that minimizes the impact of path loss while ensuring that the received signals at the user are constructive. This approach leads to a two-stage algorithm: in the first stage, the locations of the pinching antennas are optimized to minimize the large-scale path loss; in the second stage, the antenna locations are refined to maximize the received signal strength. Simulation results show that pinch-antenna systems significantly outperform conventional fixed-location antenna systems, and the proposed algorithm achieves nearly the same performance as the highly complex exhaustive search-based benchmark.**

***Index Terms*—Pinching antenna, flexible-antenna system, downlink rate maximization, line-of-sight communication.**

I. Introduction

Recently, flexible-antenna systems, such as fluid-antenna systems and movable-antenna systems, have been studied for their advantages in reconfiguring wireless channels [1], [2]. Unlike traditional fixed-antenna systems, flexible-antenna systems provide the ability to adjust antenna locations at the transceiver, thus improving channel conditions for the transceivers [3], [4]. However, in traditional flexible-antenna systems, antenna movement is limited to the wavelength scale, resulting in limited influence on large-scale path loss, which limits their applications in various scenarios. Recently, the pinching antenna has been proposed as a more promising flexible antenna system to overcome the bottlenecks in conventional flexible antenna systems [5], [6]. Specifically, by using a dielectric waveguide as a transmission medium, pinching antennas can be dynamically activated at any point along the waveguide by simply adding separate dielectric materials, thereby enabling highly flexible antenna deployment. In addition, compared to conventional flexible antennas, the pinch antenna system is less expensive and easier to install because the pinching mechanism involves simply adding or removing dielectric materials, making it well-suited for environments where system adaptability and cost-effectiveness are critical, such as industrial Internet of Things (IoT) or urban deployments.

Y. Xu is with the School of Science and Engineering, The Chinese University of Hong Kong, Shenzhen, 518172, China (email: xuyanqing@cuhk.edu.cn).

Z. Ding is with Khalifa University, Abu Dhabi, UAE. (email: zhiguo.ding@ieee.org).

G. K. Karagiannidis is with the Department of Electrical and Computer Engineering, Aristotle University of Thessaloniki, 541 24 Thessaloniki, Greece (e-mail: geokarag@auth.gr).

Z. Ding is the corresponding author.

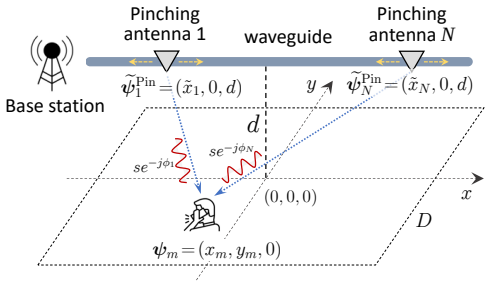

Fig. 1: A pinching-antenna system with N pinching antennas.

In this paper, we consider a downlink pinching-antenna system, where multiple pinching antennas are deployed on a waveguide to serve a single-antenna user, as shown in Fig. 1. Our goal is to maximize the downlink transmission data rate by optimizing the locations of the pinching antennas. However, the associated problem is very challenging to solve because the pinching antenna locations affect both the path losses and the phase shifts of the user's effective channel gain. To tackle this challenge and solve the formulated problem in a low-complexity manner, a relaxed optimization problem that minimizes the impact of path loss while ensuring that the received signals at the user are constructive is developed. This approach leads to a two-stage algorithm: in the first stage, the locations of pinching antennas are optimized to minimize the large-scale path loss; in the second stage, the antenna locations are refined to maximize the receive signal strength. The challenge for the addressed optimization problem can be reflected by the fact that the problem to be solved in the first stage is still nonconvex and difficult to handle. Intriguingly, we theoretically reveal that the objective function of this problem is unimodal. Leveraging this revealed property, a globally optimal solution of the antenna locations is obtained in closed-form. Then, with the obtained locations, a succinct location refinement scheme is proposed to guarantee the constructive signal receptions at the user. Simulation results demonstrate that pinching-antenna systems significantly outperform conventional fixed-location antenna systems and the proposed algorithm achieves nearly the same performance as the high complexity exhaustive search-based benchmark.

II. System Model and Problem Formulation

Consider a downlink communication system, where a base station (BS) with N antennas serves a single-antenna mobile user. The user is randomly deployed within a square area of side length D, as illustrated in Fig. 1.

A. Conventional Antenna System

We first consider the conventional antenna system, where the N BS antennas are deployed at a fixed location. Without loss of generality, we assume that the BS antennas are

deployed right above the centroid of the square area with a height d. The location of the n-th antenna is denoted by $\bar{\psi}_n = [\bar{x}_n, 0, d], \forall n \in \mathcal{N} \triangleq \{1, ..., N\}$. The spacing between two neighboring antennas is set as Δ to avoid antenna coupling. According to the spherical wave channel model [7], the channel vector between the fixed antennas and the user is given by

$$\mathbf{h}^{\mathrm{Conv}} = \left[\frac{\eta^{\frac{1}{2}} e^{-j\frac{2\pi}{\lambda}\|\boldsymbol{\psi}_m - \bar{\boldsymbol{\psi}}_1\|}}{\|\boldsymbol{\psi}_m - \bar{\boldsymbol{\psi}}_1\|}, ..., \frac{\eta^{\frac{1}{2}} e^{-j\frac{2\pi}{\lambda}\|\boldsymbol{\psi}_m - \bar{\boldsymbol{\psi}}_N\|}}{\|\boldsymbol{\psi}_m - \bar{\boldsymbol{\psi}}_N\|} \right]^\top, \quad (1)$$

where $\boldsymbol{\psi}_m = [x_m, y_m, 0]$ represents the location of the mobile user, $\eta = \frac{c}{4\pi f_c}$ is a constant where c denotes the speed of light, f_c is the carrier frequency, and λ is the wavelength in free space. The achievable data rate in the conventional antenna system is given by

$$R^{\mathrm{Conv}} = \log\left(1 + \frac{P\|\mathbf{h}^{\mathrm{Conv}}\|_2^2}{\sigma_w^2}\right). \quad (2)$$

where P is the transmit power, and σ_w^2 is the power of the additive white Gaussian noise at the user.

B. Pinching-Antenna Systems

The considered pinching-antenna system is shown in Fig. 1, where N pinching antennas are mounted on a waveguide to jointly serve the user. The waveguide is aligned parallel to the x-axis at a height d. The transmit signal is represented by s, while the phase shift of the signal received from the n-th pinching antenna is denoted by $\phi_n, \forall n \in \mathcal{N}$, and the locations of the user and the pinching antennas are denoted by $\boldsymbol{\psi}_m$ and $\widetilde{\boldsymbol{\psi}}_n^{\mathrm{Pin}}, \forall n \in \mathcal{N}$, respectively. In pinching-antenna systems, the antennas can be flexibly relocated along the waveguide over distances significantly larger than the wavelength, allowing them to be placed in close to the user. The channel vector between the pinching antennas and the user can be written as

$$\mathbf{h}^{\mathrm{Pin}} = \left[\frac{\eta^{\frac{1}{2}} e^{-j\frac{2\pi}{\lambda}\|\boldsymbol{\psi}_m - \widetilde{\boldsymbol{\psi}}_1^{\mathrm{Pin}}\|}}{\|\boldsymbol{\psi}_m - \widetilde{\boldsymbol{\psi}}_1^{\mathrm{Pin}}\|}, ..., \frac{\eta^{\frac{1}{2}} e^{-j\frac{2\pi}{\lambda}\|\boldsymbol{\psi}_m - \widetilde{\boldsymbol{\psi}}_N^{\mathrm{Pin}}\|}}{\|\boldsymbol{\psi}_m - \widetilde{\boldsymbol{\psi}}_N^{\mathrm{Pin}}\|} \right]^\top, \quad (3)$$

Unlike in (1), the locations of the pinching antennas are adjustable, meaning that $\tilde{x}_n$ can be optimized to enhance the channel conditions. The received signal at the user is given by

$$y^{\mathrm{Pin}} = \sqrt{\frac{P}{N}} (\mathbf{h}^{\mathrm{Pin}})^\top \mathbf{s} + w. \quad (4)$$

Here, the transmit power is reduced to $\frac{P}{N}$, as the total transmit power is evenly distributed among the N active pinching antennas. On the other hand, since all N pinching antennas are deployed along the same waveguide, the signal transmitted by one antenna is essentially a phase-shifted version of the signal transmitted by another [8]. Consequently, the signal vector $\mathbf{s}$ can be represented as follows:

$$\mathbf{s} = [e^{-j\theta_1}, ..., e^{-j\theta_N}]^\top s, \quad (5)$$

where s is the signal passed on the waveguide, and $\theta_n = 2\pi \frac{|\boldsymbol{\psi}_0^{\mathrm{Pin}} - \widetilde{\boldsymbol{\psi}}_n^{\mathrm{Pin}}|}{\lambda_g}$. Here, $\boldsymbol{\psi}_0^{\mathrm{Pin}}$ denotes the location of the feed point of the waveguide, and $\lambda_g = \frac{\lambda}{n_{\mathrm{neff}}}$ denotes the guided wavelength with n_{neff} signifying the effective refractive index of a dielectric waveguide [8].

Based on the above model, the received signal at the user can be written as

$$y^{\mathrm{Pin}} = \left(\sum_{n=1}^{N} \frac{\eta^{\frac{1}{2}} e^{-j\left(\frac{2\pi}{\lambda}\|\boldsymbol{\psi}_m - \tilde{\boldsymbol{\psi}}_n^{\mathrm{Pin}}\| + \theta_n\right)}}{\|\boldsymbol{\psi}_m - \tilde{\boldsymbol{\psi}}_n^{\mathrm{Pin}}\|} \right) \sqrt{\frac{P}{N}} s + w. \quad (6)$$

The system model in (6) highlights a special feature of pinching antennas. Unlike conventional antennas, pinching antennas allow reconfiguration of both the large scale path loss $|\boldsymbol{\psi}_m - \widetilde{\boldsymbol{\psi}}_n^{\mathrm{Pin}}|$ and the phase shifts θ_n by adjusting their positions, thus providing additional degrees of freedom. Using this model, the achievable data rate for the pinching antenna system can be expressed as

$$R^{\mathrm{Pin}} = \log\left(1 + \left| \sum_{n=1}^{N} \frac{\eta^{\frac{1}{2}} e^{-j\left(\frac{2\pi}{\lambda}\|\boldsymbol{\psi}_m - \widetilde{\boldsymbol{\psi}}_n^{\mathrm{Pin}}\| + \theta_n\right)}}{\|\boldsymbol{\psi}_m - \widetilde{\boldsymbol{\psi}}_n^{\mathrm{Pin}}\|} \right|^2 \frac{P}{N\sigma_w^2}\right). \quad (7)$$

The goal of this paper is to maximize the downlink data rate by optimizing the locations of the pinching antennas. The associated optimization problem can be formulated as

$$\max_{\tilde{x}_1, ..., \tilde{x}_n} \; R^{\mathrm{Pin}} \quad (8a)$$

$$\text{s.t. } |\tilde{x}_n - \tilde{x}_{n'}| \geq \Delta, \forall n, n' \in \mathcal{N}, \quad (8b)$$

where constraints (8b) guarantee that the antenna spacings should be no smaller than the minimum guide distance, Δ, to avoid the antenna coupling.

Without loss of generality, we assume that the pinching antennas are deployed in a successive order, which means

$$\tilde{x}_n - \tilde{x}_{n-1} > 0, \forall n \in \mathcal{N}. \quad (9)$$

As a result, the nonconvex constraints (8b) can be simplified as the following linear constraints:

$$\tilde{x}_n - \tilde{x}_{n-1} \geq \Delta, \forall n \in \mathcal{N}, \quad (10)$$

Meanwhile, we note that maximize the downlink data rate is equivalent to maximize the signal-to-noise ratio. Therefore, problem (8) can be equivalently recast as follows:

$$\max_{\tilde{x}_1, ..., \tilde{x}_n} \; \left| \sum_{n=1}^{N} \frac{e^{-j\phi_n}}{\|\boldsymbol{\psi}_m - \widetilde{\boldsymbol{\psi}}_n^{\mathrm{Pin}}\|} \right| \quad (11a)$$

$$\text{s.t. } \tilde{x}_n - \tilde{x}_{n-1} \geq \Delta, \forall n \in \mathcal{N}, \quad (11b)$$

$$\phi_n = \frac{2\pi}{\lambda}\|\boldsymbol{\psi}_m - \widetilde{\boldsymbol{\psi}}_n^{\mathrm{Pin}}\| + \theta_n, \forall n \in \mathcal{N}. \quad (11c)$$

However, problem (11) is still challenging to solve because the locations of the pinching antennas affect both the numerators and denominators of the objective function, and also it is shown in the exponent of the complex-valued numbers. In the next section, we will propose an efficient algorithm to handle this problem.

III. Proposed Algorithm to Solve Problem (11)

Looking at the objective function of the problem (11), we can see that the locations of the pinch antennas affect two key aspects of the channel. One is the large scale path loss, and the other is the phase shifts due to signal propagation inside and outside the waveguide. To maximize the objective function, we need to minimize the impact of the large scale

path loss associated with the terms, $|\boldsymbol{\psi}_m - \widetilde{\boldsymbol{\psi}}_n^{\mathrm{Pin}}|, \forall n \in \mathcal{N}$, on the denominator. Meanwhile, we also need to constructively combine the received signals from different pinching antennas at the user. To achieve this goal, we consider the following relaxed problem:

$$\max_{\tilde{x}_1,\ldots,\tilde{x}_n} \sum_{n=1}^{N} \frac{1}{\|\boldsymbol{\psi}_m - \widetilde{\boldsymbol{\psi}}_n^{\mathrm{Pin}}\|} \tag{12a}$$

$$\text{s.t. } \tilde{x}_n - \tilde{x}_{n-1} \geq \Delta, \forall n \in \mathcal{N}, \tag{12b}$$

$$\phi_n - \phi_{n-1} = 2k\pi, \forall n \in \mathcal{N}, \tag{12c}$$

where the objective function is to minimize the effects of large scale path loss by maximizing the sum of the reciprocals of the distances, and the constraint (12c) ensures that the received signals from different pinching antennas can be constructively combined at the user, where k is an arbitrary integer. Although problem (12) is not strictly equivalent to problem (11), our simulation results in section IV show that solving problem (12) achieves almost the same performance as the optimal solution of problem (11).

Another important observation is that to satisfy constraints (12c), one only needs to move the pinch antennas on the wavelength scale, which is much smaller than the distances between the pinch antennas and the user. Based on this insight, we design a low-complexity two-stage algorithm to solve the (12) problem. Specifically, in the first stage, we aim to maximize the sum of the reciprocals of the distances from the pinching antennas to the user under the antenna spacing constraints. Then, in the second stage, we refine the pinching antenna locations to satisfy the constraints (12c) by moving them on the wavelength scale. The details of the algorithm are described in the next two subsections.

A. Maximize the Summation of Reciprocals of Distances

The problem of maximizing the summation of reciprocals of distances under the antenna spacing constraints is given by

$$\max_{\tilde{x}_1,\ldots,\tilde{x}_n} \sum_{n=1}^{N} \left[(\tilde{x}_n - x_m)^2 + C\right]^{-\frac{1}{2}} \tag{13a}$$

$$\text{s.t. } \tilde{x}_n - \tilde{x}_{n-1} \geq \Delta, \forall n \in \mathcal{N}, \tag{13b}$$

where $C = y_m^2 + d^2 > 0$. An interesting property of the optimal solutions of problem (13) is provided in the following lemma.

Lemma 1 *With the optimal solution of problem* (13)*, the constraints* (13b) *hold with equalities, i.e.,*

$$\tilde{x}_n^* - \tilde{x}_{n-1}^* = \Delta, \forall n \in \mathcal{N}, \tag{14}$$

Proof: See Appendix A. ■

With Lemma 1, problem (13) can be simplified as

$$\max_{\tilde{x}_1} \sum_{n=1}^{N} \left[(\tilde{x}_1 + (n-1)\Delta - x_m)^2 + C\right]^{-\frac{1}{2}}. \tag{15}$$

Therefore, the original problem in (13) which is related to multiple optimization variables can be reduced to a simplified with respect to the location of the first pinching antenna only. However, problem (15) is still nonconvex with respect to $\tilde{x}_1$ and hence challenging to solve. Intriguingly, the following lemma reveals that problem (15) has a special structure, which paves the way to obtain the globally optimal solution of problem (15).

Lemma 2 *The objective function of problem* (15) *is unimodal with respect to* $\tilde{x}_1$ *if* $C \geq (N-1)^2\Delta^2$*, and the optimal* $\tilde{x}_1$ *maximizing the objective function is given by*

$$\tilde{x}_1^* = x_m - \frac{N-1}{2}\Delta. \tag{16}$$

Proof: See Appendix B. ■

We note that the condition on C is mild. For instance, when $N = 8$, $f = 6$GHz and Δ is set to half a wavelength, it only requires $C \geq 0.0306$. Additionally, at higher frequencies, the value of Δ decreases, leading to a lower required value of C. According to Lemma 2, the locations of the pinching antennas can be obtained in closed-form. In particular, the location of the n-th pinching antenna is given by

$$\widetilde{\boldsymbol{\psi}}_n^{\mathrm{Pin}} = \Big[x_m - \big(\frac{N-1}{2} + n - 1\big)\Delta, 0, d\Big], \forall n \in \mathcal{N}. \tag{17}$$

B. Refine the Pinching Antenna Locations to Satisfy (12c)

The remaining of the optimization procedure is to refine the pinching antenna locations to satisfy (12c), such that signals sent by different pinching antennas are constructively combined at the user. Here, we use a modified approach based on the one proposed in [6, Subsection III-A]. The detailed descriptions are as follows, where the case that N is an odd number is focused on for illustration purposes.

- According to Lemma 2, the obtained location of the $(\frac{N+1}{2})$-th pinching antenna is set as $[x_m, 0, d]$.
- Next, the location of the $(\frac{N+1}{2}+1)$-th pinching antenna is refined. In particular, we concentrate on the segment between $[x_m + \Delta, 0, d]$ and the end of the waveguide by using the first-obtained location which satisfies $\mathrm{mod}\{\phi_{\frac{N+1}{2}} - \phi_{\frac{N+1}{2}+1}, 2\pi\} = 0$, where $\mathrm{mod}\{a, b\}$ signifies the module operation of a by b.
- In a successive manner, the location of the n-th ($n > \frac{N+1}{2}+1$) pinching antenna can be obtained by focusing on the segment between $[\tilde{x}_{n-1} + \Delta, 0, d]$ and the end of the waveguide by using the previously obtained location which satisfies $\mathrm{mod}\{\phi_{n-1} - \phi_n, 2\pi\} = 0$.
- The locations of the pinching antennas $n < \frac{N+1}{2}$ can be found successively by following the same steps as above.

This scheme also applies to the case in which N is an even number. Specifically, the location of the $\frac{N}{2}$-th pinching antenna is initially fixed based on Lemma 2. Then, the locations of the remaining pinching antennas can be determined sequentially as outlined above.

IV. Simulation Results

In this section, the performances of the pinching-antenna systems and the proposed algorithm are evaluated via computer simulations. Without loss of generality, the same choices of the system parameters as in [6] are used, e.g., the noise

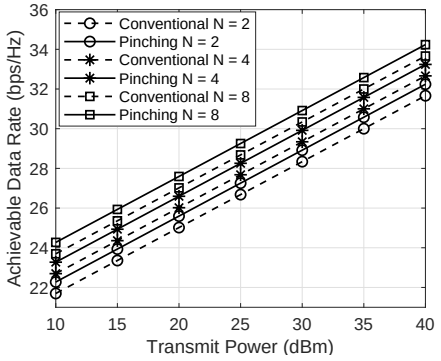

Fig. 2: Data rates of the pinching-antenna and the conventional antenna systems versus transmission powers with $D = 5$ meters.

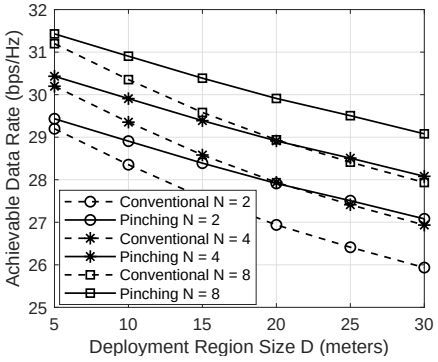

Fig. 3: Data rates of the pinching-antenna and the conventional antenna systems versus side lengths with $P = 30$ dBm.

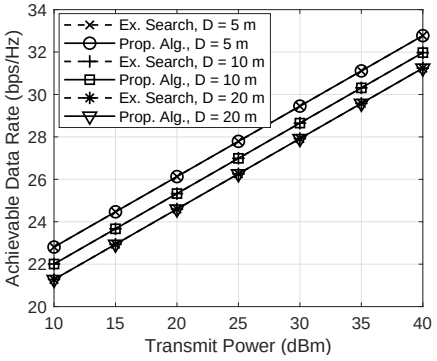

Fig. 4: Data rates of the proposed algorithm and the exhaustive search-based method for the pinching-antenna system with $N = 2$.

power is set to -90 dBm, $f_c = 6$ GHz, $d = 3$ meters, $\Delta = \frac{\lambda}{2}$, and $n_{\text{neff}} = 1.4$. While the transmission power P, the side length (D) of the square area, and the number of pinching antennas N are specified in each figure.

Fig. 2 is provided to validate the advantages of the pinching-antenna system compared to the conventional antenna system with fixed antenna positions by using the ergodic achievable data rate as the performance metric As depicted in Fig. 2, pinching-antenna systems provide higher data rates compared to conventional antenna systems. This performance gain comes from the fact that the pinching-antenna system ensure that the pinching antennas can be flexibly deployed to the ideal locations which reduce the large-scale path loss. Meanwhile, the achievable data rate increases with the number of antennas for both the pinching-antenna and conventional antenna systems, thanks to the additional degrees of freedom provided by using more antennas. However, it is worthy to point out that adding extra antennas in conventional antenna systems is not straightforward, whereas the pinching-antenna system offers superior flexibility to reconfigure the antenna system.

In Fig. 3, the performance of the pinching-antenna systems with respect to the size of the user's deployment region is evaluated. As can be observed from the figure, the achievable data rates of both antenna systems decrease with increasing D, due to larger path losses. It is also observed that the performance gap between the pinching-antenna systems and the conventional antenna systems increases with D, which not only shows the great flexibility of pinching-antenna systems to compensate path losses, but also demonstrates the robustness of the pinching-antenna system to the diverse user deployment.

To better evaluate the performance of the proposed algorithm for solving problem (11), the exhaustive search method is used as a benchmark in Fig. 4. Specifically, the exhaustive search method solves problem (11) by searching all possible locations of the pinching antennas on the waveguide with a step size of $\frac{\lambda}{50}$. Since the complexity of the exhaustive search method increases quickly with the number of pinching antennas, we focus on the special case with $N = 2$ pinching antennas in Fig. 4. This figure shows that the proposed algorithm achieves almost the same performance as the optimal solution, confirming the efficacy of the proposed scheme, which first minimizes the effects of path loss and then refines the pinching antenna locations to ensure constructive signal combination at the user.

V. Conclusions

In this work, we have studied the downlink rate maximization problem in a pinching-antenna system, where N pinching antennas are deployed on a waveguide to serve a single-antenna user. Since the pinching antenna locations affect both the path losses and the phase shifts of the user's effective channel gain, the problem is quite challenging to solve. To address this issue, we have proposed to consider a relaxed problem and solved it with a two-stage algorithm in a low-complexity manner. Simulation results have demonstrated that the considered pinching-antenna system significantly outperforms conventional fixed-location antenna systems, and the proposed algorithm achieves nearly the same performance as the high-complexity exhaustive search-based benchmark.

Appendix A
Proof of Lemma 1

Lemma 1 can be proved by using contradictions. Without loss of generality, we assume that $\tilde{x}_n^* - \tilde{x}_{n-1}^* > \Delta$.

- If $\tilde{x}_n^* + \tilde{x}_{n-1}^* \leq 2x_m$, we can move the $(n-1)$-th antenna towards the n-th antenna with a length $\delta_1 > 0$, such that $\tilde{x}_n^* - (\tilde{x}_{n-1}^* + \delta_1) = \Delta$ and $\tilde{x}_{n-1} + \delta_1 < x_m$. Meanwhile, we keep the locations of other pinching antennas unchanged. With the new location $\tilde{x}_{n-1} + \delta_1$, the $(n-1)$-th term of the objective function, $(\tilde{x}_{n-1} - x_m)^2 + C$, decreases. Therefore, the objective function value increases.
- If $\tilde{x}_n^* + \tilde{x}_{n-1}^* \geq 2x_m$, we can similarly show that by moving the n-th antenna to location $\tilde{x}_n^* - \delta_2$ with $\delta_2 > 0$, such that $(\tilde{x}_n^* - \delta_2) - \tilde{x}_{n-1}^* = \Delta$ and $\tilde{x}_n^* - \delta_2 > x_m$, the objective function value increases.

In summary, if the obtained solutions do not make constraints (13b) hold with equalities, one can always find another set of locations such that constraints (13b) hold with equalities and the objective function value increases. The proof of the lemma is complete. ■

Appendix B
Proof of Lemma 2

To prove Lemma 2, let's first define

$$g(\tilde{x}_1) \triangleq \sum_{n=1}^{N} h_n(\tilde{x}_1) = \sum_{n=1}^{N} \left[(\tilde{x}_1 + (n-1)\Delta - x_m)^2 + C\right]^{-\frac{1}{2}}. \quad (18)$$

The first-order derivative of $g(\tilde{x}_1)$ is given by

$$g'(\tilde{x}_1)=\sum_{n=1}^{N} h_n'(\tilde{x}_1)=\sum_{n=1}^{N} \frac{-(\tilde{x}_1+(n-1)\Delta-x_m)}{\left[(\tilde{x}_1+(n-1)\Delta-x_m)^2+C\right]^{\frac{3}{2}}}. \quad (19)$$

Next, we prove that $g(\tilde{x}_1)$ is unimodal with $\tilde{x}_1$ in three steps:

1) $g'(x_m-\frac{N-1}{2}\Delta)=0$: By inserting $\tilde{x}_1=x_m-\frac{N-1}{2}\Delta$ into $g'(\tilde{x}_1)$, we have

$$\begin{aligned} g'(x_m-\frac{N-1}{2}\Delta) &= \sum_{n=1}^{N} h_n'\Big(x_m-\frac{N-1}{2}\Delta\Big) \\ &= \sum_{n=1}^{N} \frac{\big(\frac{N+1}{2}-n\big)\Delta}{\left[\big((n-\frac{N+1}{2})\Delta\big)^2+C\right]^{\frac{3}{2}}}. \end{aligned} \quad (20)$$

It is straightforward to show from (20) that $h_n'\big(x_m-\frac{N-1}{2}\Delta\big)=-h_{N-n+1}'\big(x_m-\frac{N-1}{2}\Delta\big)$. For the case that N is an even number, it is clear that $g'(x_m-\frac{N-1}{2}\Delta)=0$. For the case that N is an odd number, we have $h_{\frac{N+1}{2}}'\big(x_m-\frac{N-1}{2}\Delta\big)=0$, and thus we have $g'(x_m-\frac{N-1}{2}\Delta)=0$. Summarily, $g'(x_m-\frac{N-1}{2}\Delta)=0$ always holds.

2) $g'(\tilde{x}_1)>0$ for $\tilde{x}_1<x_m-\frac{N-1}{2}\Delta$, if $C\geq(N-1)^2\Delta^2$: For $\tilde{x}_1<x_m-\frac{N-1}{2}\Delta$, first introduce a parameter $\delta_3>0$, such that $\tilde{x}_1=x_m-\frac{N-1}{2}\Delta-\delta_3$. The first-order derivative of $g(\tilde{x}_1)$ is given by

$$\begin{aligned} g'(\tilde{x}_1) &= g'\Big(x_m-\frac{N-1}{2}\Delta-\delta_3\Big) \\ &= \sum_{n=1}^{N} h_n'\Big(x_m-\frac{N-1}{2}\Delta-\delta_3\Big) \\ &= \sum_{n=1}^{N} \frac{\big(\frac{N+1}{2}-n\big)\Delta+\delta_3}{\left[\big((n-\frac{N+1}{2})\Delta-\delta_3\big)^2+C\right]^{\frac{3}{2}}}. \end{aligned} \quad (21)$$

Without loss of generality, we assume $n<\frac{N+1}{2}$, and we have

$$h_n'\Big(x_m-\frac{N-1}{2}\Delta-\delta_3\Big)=\frac{\big(\frac{N+1}{2}-n\big)\Delta+\delta_3}{\left[\big((\frac{N+1}{2}-n)\Delta+\delta_3\big)^2+C\right]^{\frac{3}{2}}}, \quad (22)$$

$$h_{N-n+1}'\Big(x_m-\frac{N-1}{2}\Delta-\delta_3\Big)=\frac{\big(n-\frac{N+1}{2}\big)\Delta+\delta_3}{\left[\big((\frac{N+1}{2}-n)\Delta-\delta_3\big)^2+C\right]^{\frac{3}{2}}}. \quad (23)$$

To let $g'(\tilde{x}_1)>0$ for $\tilde{x}_1<x_m-\frac{N-1}{2}\Delta$, it suffices to show $h_n'\big(x_m-\frac{N-1}{2}\Delta-\delta_3\big)+h_{N-n+1}'\big(x_m-\frac{N-1}{2}\Delta-\delta_3\big)>0, \forall n\in\mathcal{N}$. It is noted that, since $\frac{N+1}{2}-n>0$, we have $h_n'\big(x_m-\frac{N-1}{2}\Delta-\delta_3\big)>0$ always hold. Meanwhile, if $\big(n-\frac{N+1}{2}\big)\Delta+\delta_3>0$, we have $h_{N-n+1}'\big(x_m-\frac{N-1}{2}\Delta-\delta_3\big)>0$, and thus $g'(\tilde{x}_1)>0$. Consequently, we only need to focus on the case that $0\leq\delta_3\leq\big(\frac{N+1}{2}-n\big)\Delta$, and the condition is equivalent to showing $\big(h_n'(x_m-\frac{N-1}{2}\Delta-\delta_3)\big)^2-\big(h_{N-n+1}'(x_m-\frac{N-1}{2}\Delta-\delta_3)\big)^2>0, \forall n\in\mathcal{N}$. For ease of notation, denote $z=(\frac{N+1}{2}-n)\Delta>0$. Then, we have

$$\begin{aligned} &\Big(h_n'\big(x_m-\frac{N-1}{2}\Delta-\delta_3\big)\Big)^2-\Big(h_{N-n+1}'\big(x_m-\frac{N-1}{2}\Delta-\delta_3\big)\Big)^2 \\ &= \frac{(z+\delta_3)^2}{\left[(z+\delta_3)^2+C\right]^3}-\frac{(z-\delta_3)^2}{\left[(z-\delta_3)^2+C\right]^3} && (24a) \\ &\triangleq (z+\delta_3)^2\left[(z-\delta_3)^2+C\right]^3-(z-\delta_3)^2\left[(z+\delta_3)^2+C\right]^3 && (24b) \\ &= 4z\delta_3\left[C^3-(z^2-\delta_3^2)^2(2z^2+2\delta_3^2+3C)\right] && (24c) \\ &\triangleq C^3-(z^2-\delta_3^2)^2(2z^2+2\delta_3^2+3C) && (24d) \\ &> C^3-(z^2+\delta_3^2)^2(2z^2+2\delta_3^2+3C) && (24e) \\ &= C^3-3C(z^2+\delta_3^2)^2-2(z^2+\delta_3^2)^3\triangleq f(C) && (24f) \end{aligned}$$

where $a\triangleq b$ means a and b have the same sign. By verifying the first-order derivative, it is not difficult to see that $f(C)$ is monotonically increasing with C as long as

$$3C^2-3(z^2+\delta_3^2)^2>0 \;\Leftrightarrow\; C>z^2+\delta_3^2. \quad (25)$$

Meanwhile, one can also verify that when $C=2(z^2+\delta_3^2)$, we have

$$\begin{aligned} f(C) &= C^3-3C(z^2+\delta_3^2)^2-2(z^2+\delta_3^2)^3 \\ &= 8(z^2+\delta_3^2)^3-6(z^2+\delta_3^2)^3-2(z^2+\delta_3^2)^3=0. \end{aligned} \quad (26)$$

Combining (25) and (26), we have that $f(C)\geq 0$ if $C\geq 2(z^2+\delta_3^2)$. Since $0\leq\delta_3\leq z$, it suffices to set

$$C\geq 4z^2\geq(N-1)^2\Delta^2. \quad (27)$$

Since $h_n'(\cdot)$ and $h_{N-n+1}'(\cdot)$ are symmetry, the same conclusion can be made to the case $n>\frac{N+1}{2}$. Therefore, we have $g'\big(x_m-\frac{N-1}{2}\Delta-\delta_3\big)>0$ for the case that N is an even number. While for the case that N is an odd number, we have

$$h_{\frac{N+1}{2}}'\Big(x_m-\frac{N-1}{2}\Delta-\delta_3\Big)=\frac{\delta_3}{\big(\delta_3^2+C\big)^{\frac{3}{2}}}>0. \quad (28)$$

Therefore, $g'\big(x_m-\frac{N-1}{2}\Delta-\delta_3\big)>0$ can be established for the case that N is an odd number. In summary, if $C\geq(N-1)^2\Delta^2$, $g'(\tilde{x}_1)>0$ always hold for $\tilde{x}_1<x_m-\frac{N-1}{2}\Delta$. This indicates that $g(\tilde{x}_1)$ is monotonically increasing for $\tilde{x}_1<x_m-\frac{N-1}{2}\Delta$.

3) $g'(\tilde{x}_1)<0$ for $\tilde{x}_1<x_m-\frac{N-1}{2}\Delta$, if $C\geq(N-1)^2\Delta^2$: Similar to step 2), we can prove that $g'(\tilde{x}_1)$ is strictly negative for $\tilde{x}_1>x_m-\frac{N-1}{2}\Delta$ if $C\geq(N-1)^2\Delta^2$. This means that $g(\tilde{x}_1)$ is a monotonically decreasing function for $\tilde{x}_1>x_m-\frac{N-1}{2}\Delta$.

Combining the conclusions from the steps 2) and 3), we conclude that $g(\tilde{x}_1)$ is a unimodal function with respect to $\tilde{x}_1$ if $C\geq(N-1)^2\Delta^2$, and there exists a unique solution that maximizes the objective function. On the other hand, step 1) shows that $g'(x_m-\frac{N-1}{2}\Delta)=0$, which indicates that the optimal solution of problem (15) is $\tilde{x}_1^*=x_m-\frac{N-1}{2}\Delta$. The proof of the lemma is complete. ■

REFERENCES

[1] K.-K. Wong, A. Shojaeifard, K.-F. Tong, and Y. Zhang, "Fluid antenna systems," *IEEE Trans. Wireless Commun.*, vol. 20, no. 3, pp. 1950–1962, 2020.

[2] L. Zhu, W. Ma, and R. Zhang, "Movable antennas for wireless communication: Opportunities and challenges," *IEEE Commun. Mag.*, vol. 62, no. 6, pp. 114–120, 2024.

[3] K.-K. Wong and K.-F. Tong, "Fluid antenna multiple access," *IEEE Trans. Wireless Commun.*, vol. 21, no. 7, pp. 4801–4815, 2021.

[4] L. Zhu, W. Ma, B. Ning, and R. Zhang, "Movable-antenna enhanced multiuser communication via antenna position optimization," *IEEE Trans. Wireless Commun.*, vol. 23, no. 7, pp. 7214–7229, 2024.

[5] H. O. Y. Suzuki and K. Kawai, "Pinching antenna: Using a dielectric waveguide as an antenna," *NTT DOCOMO Technical J.*, Jan. 2022.

[6] Z. Ding, R. Schober, and H. V. Poor, "Flexible-antenna systems: A pinching-antenna perspective," *submitted for publication*, 2024.

[7] H. Zhang, N. Shlezinger, F. Guidi, D. Dardari, M. F. Imani, and Y. C. Eldar, "Beam focusing for near-field multiuser MIMO communications," *IEEE Trans. Wireless Commun.*, vol. 21, no. 9, pp. 7476–7490, 2022.

[8] D. M. Pozar, *Microwave engineering: theory and techniques*. John wiley & sons, 2021.